

## Performance Measures of Positive Output Superlift Luo Converter Using Multitudinous Controller

P. Sivagami<sup>1</sup>, N. M. Jothi Swaroopan<sup>2</sup>

<sup>1</sup>Departement of Electrical and Electronics Engineering, Sathyabama Institute of Science and Technology ,Chennai

<sup>2</sup>Departement of Electrical and Electronics Engineering, Engineering, RMK Engineering College ,Chennai

---

### Article Info

#### Article history:

Received Dec 17, 2017

Revised Jan 13, 2018

Accepted Jan 27, 2018

---

#### Keyword:

Current controller

Positive output elementary

Super lift LUO (POESLL)

Sliding mode controller(SMC)

---

### ABSTRACT

In order to meet the increase in energy demand globally it is necessary to harness renewable energy at its maximum potential for the purpose of electric power generation. For the achievement of high output voltage and efficiency DC-DC converters plays a vital role in low voltage PV array and fuel cells. LUO converters are gaining importance because of geometric progression output. . LUO converters find its application because of high transient performance of the system, high power transfer gain, efficiency and reduced ripple .Because of load and line disturbances the output voltage of DC-DC converter must be operated in closed loop mode. This paper interpolates multitudinous controller for positive output elementary super lift LUO converter (POESLL). The pursuance of the converter under manifold such as variation in input, load are developed and compared for current mode controller and SMC.

*Copyright © 2018 Institute of Advanced Engineering and Science.*

*All rights reserved.*

---

### Corresponding Author:

P.Sivagami,

Departement of Electrical and Electronics Engineering,

Sathyabama Institute of Science and Technology, Chennai, India

Email: sivagamitec@gmail.com

---

## 1. INTRODUCTION

LUO converters are power optimizers as it helps in harvesting maximum energy from renewable energy systems. There are two ways in which maximum energy can be harnessed that is by using MPPT technique or by improving the controller design for DC-DC converters. Different types available such as PI, PID, current controller, SMC and intelligent controllers. In PV array fed DC-DC converter the input varies depending on temperature and irradiation. Model predictive control MPPT technique apply the switching signal by determining the error before next sampling time [1].POESLLC converter with MPPT output compared with the change in output voltage resulted between the difference of output voltage and reference voltage the power flow is maximized [2]. For selecting the best converter for PV state space averaging technique is employed for developing a circuit model for POESLL .It helps in the design of controller and determines the stability region for the proposed PV system [3]. PI controller with pulse width modulating SMC controls a third order POESLLC that suppresses the steady state error of the output voltage and also reduces the number of sensors used [4]. For a positive output super lift re lift LUO converter output feedback controller is improved by regulating the output voltage directly and it obeys the control law and overcomes the phase obstacle experienced by a boost type DC-DC converter [5]. Fuzzy logic controller is validated for re lift LUO converter for better regulation of output voltage and for effective performance [6]. LUO converter series is analyzed for voltage ripple stresses on switches. State space modeling and circuit averaging technique is developed. Bode plot, pole zero plots are obtained for open loop as well as closed loop. The stability is validated using the pole zero plot for proportional integral controller developed using Ziegler Nichols Tuning procedure [7]. The voltage at the output terminal is regulated by creating a sliding surface using sliding mode controller which drives a fuzzy inference to generate pulses using pulse width

modulation [8]. The dynamic performance is enhanced by LQR plus FLC. Two loops are considered inner current loop and output voltage loop. Inner loop regulates the inductor current and outer loop adopts FLC. The performance of the POESLLC using this controller is validated at various working conditions viz. appropriate selection of the controller gains and fuzzy rules [9]. The load estimator with the state-feedback control uses separation principle.

The desired output voltage value is tracked by proper selection of the state feedback and gain matrix for effective stability [10]. The MPPT technique is designed and implemented using an adaptive neuro fuzzy inference system for a boost converter. ANFIS and PI is used to extract the maximum power by adjusting the duty ratio of the boost converter [11]. The non-linear nature due to input and load variations is overcome by constant frequency sliding mode controller. It improves the performance and regulates the output voltage [12]. DC-DC converters are estimated based on the energy factor to obtain the model and second order transfer function for  $n$  number of capacitors and inductors [13]. Increase in the efficiency of the converter is achieved by minimizing the switching loss by operating the switch at the lower frequency than the actual. It is implemented by a specified fraction of switching periods of pass through and non pass through period. This in turn helps in reduction of the ripples [14]. The inductor current and output voltage are predicted at the same time. This is achieved by adding to the DPWM, the control variable. The closed loop stability is enhanced, power efficiency improved by means of dither generation module [15]. PID controller for POESLL is tuned based on artificial intelligent techniques compared with Ziegler Nichols method. The performance of the converter is improved using artificial intelligent techniques [16]. Because of robustness of PID controller to reject disturbances arising from supply, load variation and changes in circuit elements, the set point of PID controller is tuned by five different methods for the boost converter [17]. In 3 phase 5 level inverter fed by dc converter compares PI and FLC controller performance for regulating the current. For tracking of maximum power from the PV panel Perturb and observe Maximum Power Point Technique (MPPT) is used. Finally Total Harmonic Distortion (THD) comparison made between two controllers for validation of results [18].

## 2. LUO CONVERTER

Dramatic changes in the DC-DC conversion technique is due to industrial requirement. They are the high power density and high voltage gain. The block schematic of LUO converter fed by solar array is shown in Figure 1.

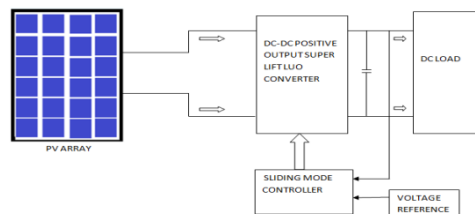


Figure 1. Block diagram representation of POESLL

The current mode control scheme is widely used; there exists a problem in sensing of the current which results in noise generation. Among different converters used in practice, the voltage transfer ratio is limited with the increase in duty cycle due to the power semiconductor switches, power diodes and the equivalent series resistance of the passive components. Moreover increase in duty cycle may result in the reverse recovery problems of the semiconductor devices. Its robustness to model uncertainties. SMC controller compared to current controller guarantees feasibility and stability. Its responsive to real and relatively fast alterations is high and so the system will be faster to reach set point. The settling time is less the SMC controller and current controller fed PV array is compared for load and line variations is presented.

## 3. WORKING OF SUPERLIFT LUO CONVERTER

The DC input from the PV array fed to LUO converter consists of capacitor  $C_1$ , connected parallel to the source,  $C_1$  connected across the load, inductor  $L_1$ , freewheeling diodes  $D1, D2$ , power switch  $S_1$ . The modes of operation of positive super lift LUO converter consists of switch ON and Switch Off mode. The voltage lift is done by the inductor  $L_1$  and the capacitor  $C_1$ . The figure 2 shows the circuit diagram of positive super lift LUO converter. In figure 3 that is during switch ON mode that is when the switch is closed, the

current across the inductor increases with the increase in voltage, the capacitors are charged to the source voltage  $V_{in}$ . The energy to the load is fed by the capacitor  $C_1$ . In Figure 4 when the switch is open the voltage across the inductor decreases with  $V_0 - 2V_{in}$ . The ripple current across the inductor is given by

$$\Delta i_{l1} = \frac{V_L - 2V_{in}}{L_1} \delta T \quad (1)$$

The voltage transfer gain is given by

$$M = \frac{V_L}{V_{in}} = \frac{2 - \delta}{1 - \delta} \quad (2)$$

$$V_L = M V_{in} \quad (3)$$

The input current during the switch on period is equal to the sum of current across the inductor  $L_1$  and capacitor  $C_i$ , but during switch off condition it is equal to current across the inductor  $L_1$ . The average charge across the capacitor will not change for the steady state conditions therefore that is on time on and off time current across the capacitor  $C_i$  must be equal. It is given by

$$\delta T i_{C_{iON}} = (1 - \delta) T i_{C_{iOFF}} \quad (4)$$

The inductor current is equal to average current for large value of  $L_1$  and during off condition it is given by

$$\dot{i}_{in} = \dot{i}_{l1} = \dot{i}_{c1} \quad (5)$$

The average input current is given by sum of the input current during the on and off time period and it is

$$i_{in} = (2 - \delta) i_{l1} \quad (6)$$

$$i_{in} = \frac{(2 - \delta)^2}{(1 - \delta)^2 R_L} \quad (7)$$

The ripple voltage across the output is given as

$$\Delta V_L = \frac{(1 - \delta) V_L}{f C_1 R_L} \quad (8)$$

The equations for state space modelling is given by state variables  $i_{L1}$ ,  $V_{ci}$ ,  $V_{cl}$  are as follows

$$L_1 \frac{di_{l1}}{dt} = \frac{i_{l1}}{R_{in}} - V_{Ci} - V_{Cl}, \quad \frac{di_{l1}}{dt} = \frac{i_{l1}}{L_1 R_{in}} - \frac{V_{Ci}}{L_1} - \frac{V_{Cl}}{L_1} \quad (9)$$

$$C_i \frac{dV_{ci}}{dt} = i_{l1}, \quad \frac{dV_{ci}}{dt} = \frac{i_{l1}}{C_i} \quad (10)$$

$$C_l \frac{dV_L}{dt} = i_{l1} - \frac{V_L}{R_l}, \quad \frac{dV_L}{dt} = \frac{i_{l1}}{C_l} - \frac{V_L}{C_l R_l} \quad (11)$$

$R_{in}$  is the internal source resistance, it is very negligible and not taken into consideration. These above statements are for ON condition. Similarly for OFF conditions the equations can be written as follows

$$L_1 \frac{di_{l1}}{dt} = V_{Ci} + V_{Cl}, \quad \frac{di_{l1}}{dt} = \frac{V_{Ci} + V_{Cl}}{L_1} \quad (12)$$

$$C_i \frac{dV_{ci}}{dt} = \frac{V_{in}}{R_{in}} - 2i_{l1}, \quad \frac{dV_{ci}}{dt} = -\frac{2i_{l1}}{C_i} + \frac{V_{in}}{R_{in}C_i} \tag{13}$$

$$C_l \frac{dV_{CL}}{dt} = i_{l1}, \quad \frac{dV_L}{dt} = \frac{i_{l1}}{C_l} \tag{14}$$

$$\begin{pmatrix} \frac{di_{l1}}{dt} \\ \frac{dV_{ci}}{dt} \\ \frac{dV_{Cl}}{dt} \end{pmatrix} = \begin{pmatrix} 0 & -\frac{1}{L_1} & -\frac{1}{L_1} \\ \frac{1}{C_i} & 0 & 0 \\ \frac{1}{C_l} & 0 & -\frac{1}{RC_l} \end{pmatrix} \begin{pmatrix} i_{l1} \\ V_{ci} \\ V_{Cl} \end{pmatrix} + \begin{pmatrix} \frac{V_{ci} + V_{Cl}}{L_1} \\ -\frac{2i_{l1}}{C_i} + \frac{V_{in}}{R_{in}C_i} \\ -\frac{i_{l1}}{C_l} \end{pmatrix} Y + \begin{pmatrix} \frac{V_{in}}{L_1} \\ 0 \\ 0 \end{pmatrix}$$

The state space modelling of the circuit is given by  $\dot{\bar{X}} = Ax + By + Cz$  (12)

The vectors of the state variables and their derivatives are  $\bar{X}$  &  $\dot{x}$ . The disturbance matrix is  $C$  and the input is  $Z$ .

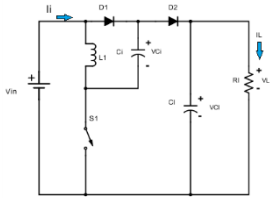


Figure 2. Circuit diagram of POESLL

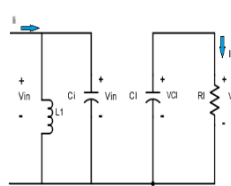


Figure 3. ON mode

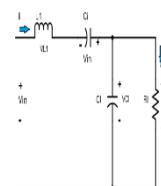


Figure 4. OFF mode

The programming code can be developed for the converter by two methods. In one method by assigning the values of input voltage, duty cycle, load resistance, efficiency %, inductor ripple current, switching frequency and % output voltage ripple. This method helps in determining the inductor value, capacitor value, input current, output power, which can be determined. In the second method the values assigned are, input voltage, inductor value, capacitor value, switching frequency, duty cycle, input resistance, load resistance. The converter output power, energy ratio, mathematical model and transfer function, rise time, settling time, damping ratio are obtained. The coding in MATLAB for the method 1 is given below.

```

clc
clear
x=menu('menu','ENTER THE VALUE','Thanks');
if(x==1);
Vin=input('Vin='); R=input('R=');
EL1=input('EL1=');
Vl=input('Vl=');
EFF=input('EFF=');
f=input('f='); k=input('k=');
t=1/f;
M=(2-k)/(1-k);
Vo=M*Vin; Io=Vo/R;
disp('Po')
Po= Vo* Io
disp('Pin')
Pin= (Po/ EFF)*100
disp('Iin')
Iin= Pin/Vin
disp('L')
L=Vin*k/(f* EL1)
disp('C1')
C1= ((1-k)* Vo) / (f* VC1*R)
disp('C2')
C2= (1-k)* Vo / (f* VC1*R)
    
```

```

IL1=( Vo/L*M);
VC1= Vin;
VC2= Vo*K/(2-K);
WL=0.5*IL1^2*L;
WC=0.5*C1*VC1^2+0.5*C2*VC2^2;
T=1/f;
Po=Vo*Io;Ploss=r*IL1^2;
Iin=(Po+Ploss)/Vin;
disp('The efficiency')
eff=abs((Vo*Io)/(Vin*Iin))
disp('pumping Energy')
PE=abs(Vin*Iin*T)
disp('Stored Energy')
SE=abs(WC+WL)
disp('Capacitor-Inductor stored Energy ratio')
CIR=abs(WC/WL)
disp('Energy Factor')
EF=abs(SE/PE)
disp('time constant')
A = [0 -1/L -1/L; 1/C1 0 0;1/C2 0 -1/R*C2]
B = [(1-k)/L; k/C1;0]
C = [0 0 1]
D =[0]
% Create a Matlab state-space model.
sys = ss(A, B, C,D);
sys = ss2tf(A, B, C,D)
[num, den] = ss2tf(A,B,C,D)
G = tf(num,den)
bode(tf(num,den))
close 'all';
% Compute and plot the step response.
figure;
[y, t] = step(sys);
plot(t, y);
title('Step Response');
% Compute and plot the impulse response.
figure;
[y, t] = impulse(sys);
plot(t, y);
title('Impulse Response');
end

```

Similarly the coding can be developed for method 2. Thus the coding can be repeated for n number of cycles by writing the program using while loop. The table I shows the design calculations for various inputs for the method 1. The assigned values are  $V_{in}$ , output ripple voltage  $\% = 0.12$ , % inductor ripple current  $\% = 0.6$ , efficiency  $\% = 92$ ,  $k = 0.5$ , switching frequency  $= 10\text{kHz}$ ,  $R = 50\ \Omega$ . The values assigned can be carried out for different duty cycle, load resistance, efficiency, switching frequency, ripple voltage, ripple current etc. From the above program transfer function, bode plot, state space model, analysis of stability can be carried out. Thus it helps in collecting data and processing it for future studies.

Table 1. Design calculations

S No	$V_{in}$ (V)	$V_{out}$ (V)	$I_{out}$ (A)	$P_{out}$ (Watts)	$C1$ ( $\mu\text{F}$ )	$C2$ ( $\mu\text{F}$ )	$L$ ( $\mu\text{H}$ )
1	12	36	0.72	25.92	30	30	100
2	36	108	2.16	233.78	90	90	300
3	52	156	3.12	486.72	130	130	430

#### 4. SIMULATION

The current controller fed with dc supply is simulated for constant input, line and load variations. In current-mode control, the sensed inductor-current ramp which is a state variable is used in generating pulses to the switches. For 12 V DC input, the simulation and output is shown in diagram Figure 5. From the output figure the peak overshoot is almost 1 ampere for current output and near 50 V for output voltage. The Figure 6 shows the line disturbances and also the output voltage and current variations due to the same. The load variation simulation and its corresponding output is shown in Figure 7. Thus the performance of current controller under line and load variations is studied. PV array with out MPPT tracking is fed to the LUO converter controlled by current controller and its output waveforms are shown in figure 8. The PV fed

current controller is simulated for 52 volt input from the array and its output is 152.3 V and its output current is 3.04 amperes and the output power is 460 watts. The components values assigned the same for both PV array and dc input .The disadvantages of this type of controller is studied from the simulation output.

SMC is designed and simulated for 12V input. The output current is 0.71 A and the output voltage is 36V. The simulation and output are shown in figure 9 for constant load of 50 ohms. Line variations in which input voltage is varied from 12V to 20V, the output remains constant inspite of these disturbances is shown in Figure 10. The load resistance is varied from 50 ohms to 100 ohms .Then also the output voltage remains the same .The simulation diagram and output is shown in Figure 11. The line variations and load disturbances are overcome by SMC that is the settling time is reduced when compared to that of the current controlled POESLL. The PV with out MPPT feeds LUO converter .It is simulated for a input of 52 V. The output voltage is 155 V, output current is 3.1 A, output power is 481 Watts. The table II Shows the comparison of simulated output and calculated output.

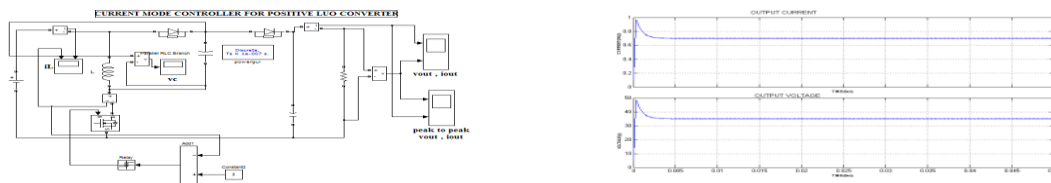


Figure 5. Simulation and output waveform of 35V for 12V input current mode controller

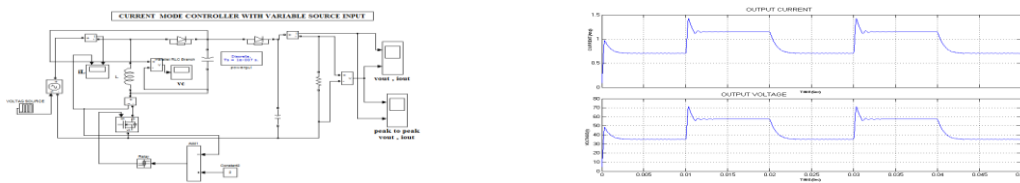


Figure 6. Simulation for line variation and output current and voltage waveform for current mode POESLL



Figure 7. Simulation for load variations and output current and voltage waveform for controlled POESLL

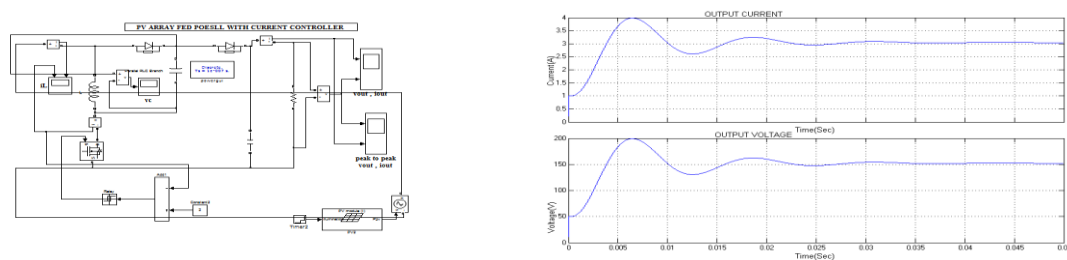


Figure 8. Simulation and output waveform for PV array current controlled POESLL

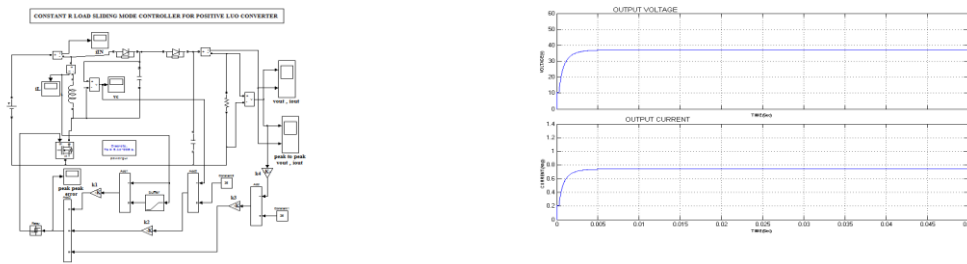


Figure 9. Simulation and output waveform of 36V for 12V input SMC controller

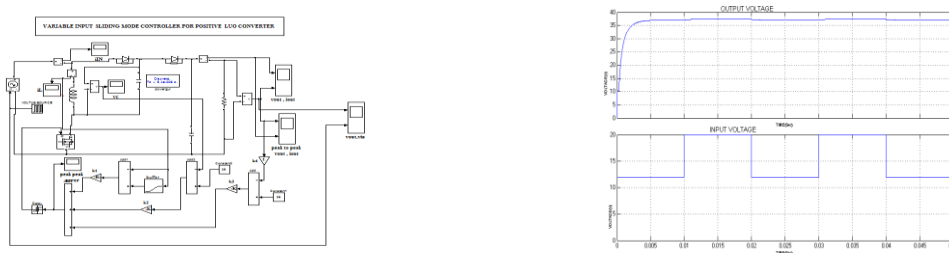


Figure 10. Simulation for line variation and output current and voltage waveform for SMC POESLL

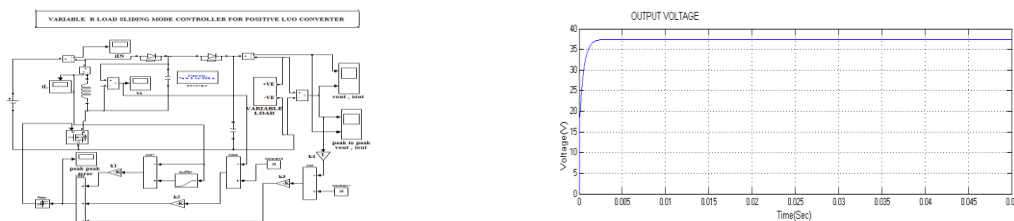


Figure 11. Simulation for load variations and output current and voltage waveform for SMC POESLL

Table 2. Comparison of simulated output and calculated output.

Controller	SIMULATED OUTPUT				CALCULATED OUTPUT		
	Vin (V)	Vout (V)	Iout (A)	Pout (Watts)	Vout (V)	Iout (A)	Pout (Watts)
CM	12	35	0.69	24.15	36	0.72	25.92
	52	152	3.03	462.992	156	3.12	486.72
SMC	12	36	0.71	25.56	36	0.72	25.92
	52	155	3.13	485.15	156	3.12	486.72

### 5. CONCLUSION

The control technique such as current controller and SMC has been presented in this paper. The code is developed to determine the design and to analyse the performance of the system. By boosting the output in geometric progression for POESLL, SMC control technique in POESLL will stabilise the output for any change in load and line variations. The error signal is produced by comparing the inductor current and

capacitor voltage with the reference value. By means of proper selection of control parameters in SMC helps in achieving better performance when compared to current controlled superlift Luo converter.

## REFERENCES

- [1] V. Usharani, et al., "Enhanced MPPT Technique For DC-DC Luo Converter Using Model Predictive Control For Photovoltaic Systems" *International Journal of Engineering Research and Development* e-ISSN: 2278-067X, p-ISSN: 2278-800X, Volume 11, Issue 01 (January 2015), PP.18-27
- [2] S. Balakumar, et al., "Implementation Of Photovoltaic MPPT With Regulated Load Power Controller For Positive Output Elementary Output Superlift LUO Converter" *International Journal Of Pure And Applied Mathematics* ISSN:1311-8080 Volume 115 No.8 2017,615-621
- [3] Sundarajan Venkatesan, et al., "Modelling And Simulation Analysis Of Solar PV Energy System With LUO Converter Using State Space Averaging Technique" *International Journal of Advanced Engineering Technology* E-ISSN0976-3945 Volume II /Issue II/April June 2016/770-777
- [4] Hadi Nasiri Jazi, et al., "PI and PWM Sliding Mode Control of POESLL Converter", *IEEE Transactions on Aerospace and Electronic Systems*, Year: 2017, Volume: 53, Issue: 5
- [5] Wentao Jiang, et al., "Improved output feedback controller design for the super-lift re-lift Luoconverter", *IET Power Electronics* Year: 2017, Volume: 10, Issue: 10, Pages: 1147 - 1155
- [6] A. Sivakumar, et al., "Implementation of intelligent fuzzy controller for Positive Output Re lift LUO converter," International Conference on Circuits, Power and Computing Technologies [ICCPCT-2014], Year: 2014 Pages: 1011 - 1017
- [7] Divya Navamani Jayachandran, et al., "Modelling and Analysis Of Voltage Mode Controlled LUO Converter", *American Journal Of Applied Sciences*
- [8] G. Alwin, et al., "An Investigation On Sliding Mode Controller With Fuzzy Inference System For A DC-DC Converter", *Journal Of Harmonized Research In Engineering*, 2(2), ISSN2347-7393 PP-266-273
- [9] N. Arunkumar, et al., "Improved Performance Of Linear Quadratic Regulator Plus Fuzzy Logic Controller For Positive Output Super-Lift LUO-Converter", *Journal of Electrical Engineering*, Year 2016
- [10] Rai Munoz; Xuejian Rong, et al., "Depth-aware indoor staircase detection and recognition for the visually impaired people" Year: IEEE International Conference on Multimedia and Expo Workshops (ICMEW) Year 2016
- [11] Ravinder K. Kharb, et al., "Design And Implementation of ANFIS based MPPT Scheme with Open Loop Boost Converter For Solar PV Module", *International Journal Of Advanced Research In Electrical Electronics And Instrumentation Engineering* Vol3, issue 1, Jan 2014
- [12] A. Goudarzian, et al., "Design And Implementation of A Constant Frequency Sliding Mode Controller For A LUO Converter", *IJE TRANSACTIONS B: Applications* Vol. 29, No. 2 (February 2016) 202-210
- [13] Ahmed Hammoda, et al., "Estimation Of Advanced Dc/Dc Luo converters based On Energy Factor And Sub-Sequential Parameters" ENERGYCON 2014 • May 13-16, 2014 • Dubrovnik, Croatia
- [14] Jones.D.C, et al., "Buck-Boost Converter Efficiency Maximization via a Nonlinear Digital Control Mapping for Adaptive Effective Switching Frequency", *Emerging and Selected Topics in Power Electronics, IEEE-2013*
- [15] Bo Li, Xuefang Lin-Shi; Bruno Allard, "A Digital Dual-State-Variable Predictive Controller for High Switching Frequency Buck Converter With Improved  $\Sigma$ -ADPWM", *IEEE Transactions on Industrial Informatics*, Volume: 8, Issue: 3, Aug. 2012
- [16] Saranya.S, et al., "Tuning of PID controller for Positive Output Elementary Super-Lift Luo-Converters using AI Techniques", *International Journal of Engineering Research & Technology (IJERT)*, ISSN-278-0181, Vol. 2 Issue 11, November – 2013
- [17] Oladimeji Ibrahim, Nor Zaihar B Yahaya, Nordin Saad, "PID Controller Response to Set-Point Change in DC-DC Converter Control", *International Journal of Power Electronics and Drive Systems (IJPEDS)* Vol 7, No 2: June 2016
- [18] M. Venkatesan, R. Rajeshwari, N. Deverajan, M. Kaliyamoorthy, "Comparative Study of Three Phase Grid Connected Photovoltaic Inverter Using PI and Fuzzy Logic Controller with Switching Losses Calculation", *International Journal of Power Electronics and Drive System (IJPEDS)* Vol. 7, No. 2, June 2016, pp. 543~550 ISSN: 2088-8694